RESEARCH PAPER

MONITORING OF CO, NO$_2$ AND SO$_2$ LEVELS DURING THE COVID-19 PANDEMIC IN IRAN USING REMOTE SENSING IMAGERY

Nurwita Mustika Sari[1,2]*, Muhammad Nur Sidiq Kuncoro[3]
[1]Department of Geography, Faculty of Mathematics and Natural Science, Universitas Indonesia
[2]Remote Sensing Application Center, LAPAN, Indonesia
[3]Department of Management, Faculty of Economics and Business, Universitas Indonesia
*Corresponding author: nurwita_sutaat@yahoo.com; nurwita.mustika@lapan.go.id

ABSTRACT. The COVID-19 pandemic has had a major impact on various sectors. Iran is one of the countries most affected by this pandemic. After considering the huge impact, the government imposed strict rules prohibiting social gatherings and restricting travel for the entire population following the large number of victims in the country. These restrictions lead to changes in the environment, especially air quality. The purpose of this study was to find out how the COVID-19 pandemic affected air quality in Iran following the activity restrictions in the region. The method used in this research was based on the use of multitemporal Sentinel-5P data processing with scripts available on the Google Earth Engine applied on the images, acquired in the period before and after the COVID-19 pandemic. The data used included the image collection of Sentinel-5P NRTI CO: Near Real-Time Carbon Monoxide, Sentinel-5P NRTI NO$_2$: Near Real-Time Nitrogen Dioxide and Sentinel-5P NRTI SO$_2$: Near Real-Time Sulphur Dioxide. The results showed, that for Iran in general, changes in the concentration of CO are clearly visible in urban areas with high population activity such as Tehran, where there was a decrease from 0.05 to 0.0286 mol/m^2, while for other areas it is also influenced by the varying climate conditions, which affect the level of pollution. For the NO$_2$ pollutant, there was a significant decrease in pollution levels in big cities such as Tehran, Qom, Isfahan and Mashhad from 0.0002 to 0.000114 mol/m^2. For the SO$_2$ pollutant, there was a decrease in pollution levels in Iran's big cities from 0.0005 to 0.0000714 mol/m^2. For Tehran province, which is the most populous and busiest province in Iran, it can be observed that there was also a decrease in the concentration of pollutants after the lockdown compared to the pre-lockdown period. The CO concentration decreased from 0.043 to 0.036 mol/m^2, while for the NO$_2$ pollutant there was a decrease from 0.0002 to 0.000142 mol/m^2 and for the SO$_2$ pollutant, there was a decrease from 0.0005 to 0.000143 mol/m^2.

KEYWORDS: COVID-19, global pandemic, Iran, air pollution, Sentinel-5P imagery

Conflict of interests: The authors reported no potential conflict of interest.

INTRODUCTION

The COVID-19 outbreak was caused by the SARS-CoV-2 novel coronavirus which appeared around the end of 2019 in the Wuhan area, Hubei Province, China. Since the emergence of this disease, various sectors were shocked many times not only medically but also economically around the world due to the ease of its transmission between humans and the resulting impact of late handling. COVID-19 has been declared a global pandemic by WHO circa March 2020, following its spread throughout the world regardless of climate, the race of population and even the development stage of the country.

Considering the situation in Iran, in late October 2020, Iran reported a death due to COVID-19 every four minutes (Reuters 2020). Not only citizens were infected, several country officials such as the leader of parliament and dozens of parliament members have tested positive for COVID-19. Following the large number of positive COVID-19 cases which is getting worse and the increasing number of victims, the Iranian government began to enact regulations related to mitigation of the COVID-19 outbreak, as has been done in many affected countries. These rules include the prohibition of social gatherings and frequent travel within the territory of the country.

Research related to COVID-19 was still limited but increasing very rapidly in various aspects because of the consequences caused by this global pandemic. The existing research was related to the characteristics, mode of transmission and origin of this COVID-19 infection (Adnan

et al. 2020); the correlation between weather variables and the pandemic in Jakarta (Tosepu et al. 2020); epidemiology and pathogenesis which also studies the transmission and phylogenetics of coronaviruses (Rothan & Byrareddy 2020); and the comparison of COVID-19 with the predecessors, SARS and MERS, which were also caused by the coronavirus (Petrosillo et al. 2020).

The pollution of air by various types of contaminants is mainly associated with motor vehicle emissions and smoke from industrial chimneys. The impact caused by air pollution includes the spread of heart diseases, which suggests a close relationship between exposure to air pollution and diseases of the cardiovascular system (Andersson et al. 2020); (Miller 2020). Its other impacts are related to mental health as it causes depressive symptoms (Altuğ et al. 2020) and the influence on the health of children due to their imperfect breathing system and immunity (Kurata et al. 2020). Another thing that also turns out to be related to air pollution is frequent traffic accidents (Wan et al. 2020).

In terms of economy and finance, air pollution can even affect the disposition of financial transactions and influence the transition from direct shopping in stores to online shopping (J. (Jie) Li et al. 2019). Research related to the effect of COVID-19 on air pollution in China has been carried out by looking at the implications of lockdown in North China (Wang et al. 2020). On the other hand, it has also been studied how the COVID-19 pandemic affects NO^2 and $PM_{2.5}$ concentrations in the US through federal air monitoring network data (Berman & Ebisu 2020). Based on this study, the COVID-19 pandemic had a major impact on behavior change, causing a reduction in NO_2 concentration by 25.5% with an absolute decrease of 4.8 ppb compared to previous years. In addition, the pandemic caused a decrease in $PM_{2.5}$ due to the closure of business activities.

Various remote sensing data have been extensively used for observing air pollution. Remote sensing was used for air pollution monitoring through the IASI (Infrared Atmospheric Sounding Interferometer) feature of the Metop series satellites, which allows to observe ammonia, sulphur dioxide (SO_2) and Ozone (O_3) pollutants (Clerbaux et al. 2017). In addition, air pollution sources were detected from MODIS remote sensing data to view aerosols in 1 km resolution using Glowworm Swarm Optimization (GSO) (Chen et al. 2017). Other studies on monitoring air pollution with remote sensing data are related to determining industrial pollution emissions from VIIRS Nightfire data (Sun et al. 2020), measuring aerosols in the metropolitan area (Vratolis et al. 2020), measuring $PM_{2.5}$ concentration with MODIS data and machine learning (X. Li & Zhang 2019), measuring air pollution from motor vehicles on urban roads (Smit et al. 2019), and detection of aerosols using MODIS data (Filonchyk et al. 2017). In another study, research of methane variability in Pakistan, Afghanistan and surrounding areas was carried out using Sciamachy/Envisat data (ul-Haq et al. 2015)

Other studies related to the use of remote sensing data for air pollution analysis are studies that look at air pollution inputs to a specific desert area, the Mojave Desert, using the airborne, in-situ and remote sensing satellite data as desert ecosystems are particularly vulnerable to pollution from urban activities. Measurement data in this study were obtained from the mobile air quality laboratory, AMOG (AutoMObile trace Gas), with additional GHG and O_3 data from AJAX – Alpha Jet Atmospheric eXperiment. Further, the aerosol modeling was carried out using LiDAR (Leifer et al. 2019). To detect vehicle emissions on roads, an on-road remote sensing system with infrared (IR) and ultraviolet (UV) bands was used, which also has a speed detector and a camera to capture the image of vehicle plates (Huang et al. 2018). Another study has predicted the concentrations of $PM_{2.5}$ using MODIS Terra and Aqua remote sensing data and dynamic spatial panel model (Fu et al. 2020). A study comparing the use of direct on-site measurements and remote sensing data for monitoring air pollution and health aspects in Canada has shown that they give similar results and are associated with each other (Prud et al. 2013).

Sentinel-5P data, which is still relatively new in monitoring air quality, was used to investigate NO_2 pollution in France (Omrani et al. 2020). In another study, Sentinel-5P was used for monitoring sulphur dioxide and nitrogen dioxide in the South African region as a result of coal-fired power plants (Shikwambana et al. 2020). TROPOMI on Sentinel-5P was used to analyse the level of NO_2 concentration in Ecuador after the COVID-19 lockdown, which emphasizes the importance of air quality for human health. From this research, a reduction of NO_2 concentrations (-13%) was observed in Ecuador (Pacheco et al. 2020).

Sentinel-5P was launched in October 2017 with a specific mission of monitoring air pollution, which is the focus of this study. This satellite is dedicated to monitoring the atmosphere with an instrument called the TROPOspheric Monitoring Instrument (TROPOMI). Its aim is to reduce gaps in the availability of global atmospheric data such as SCIAMACHY/Envisat (which ended in April 2012), the OMI/AURA mission and the future Copernicus Sentinel-4 and Sentinel-5 missions. TROPOMI combines the power of SCIAMACHY data, OMI, and state-of-the-art technology to provide observations with performance that other instruments currently cannot meet. Its advantages include higher sensitivity as well as spectral, spatial and temporal resolution (ESA 2021). That is why the use of Sentinel-5P data has a very high potential for observing air pollution conditions in a wide area and over a long period. Iran as one of the countries that have been heavily affected by the pandemic had to implement a strict lockdown to control the spread of the virus. This study aims to analyse the effect of social activity and travel restrictions due to the COVID-19 global pandemic on air pollution in Iran.

MATERIALS AND METHODS

Materials

This research focuses on the Tehran province of Iran where the capital city is located. The data used in this study includes the Sentinel-5P NRTI CO: Near Real-Time CO, Sentinel-5P NRTI NO_2: Near Real-Time NO_2 and Sentinel-5P NRTI SO_2: Near Real-Time SO_2. The dataset version used in this research is Near Real-Time, or NRTI, which covers a smaller area than the offline version but appears more quickly after acquisition. These datasets were provided by European Space Agency (ESA) and are available on Earth Engine Data Catalog developed by Google (Google 2020).

As explained by ESA, the CO pollutant dataset used is global CO data in the clear-sky and cloudy-sky conditions in the 2.3 m spectral range of the shortwave infrared (SWIR) part of the solar spectrum. Noise in the data causes negative values to appear. Negative vertical column values are often observed especially over clean regions or very low SO_2 emissions. It is stated that is recommended not to filter these negative values except for outliers, i.e., vertical columns lower than -0.001 mol/m^2. In the NO_2 data collection used, the dataset represents the collective nitrogen oxide concentration that occurs as a result of the photochemical cycle during the day involving ozone and sunlight.

The TROPOMI NO_2 processing system is based on the algorithm developments for the DOMINO-2 product and the EU QA4ECV NO_2 dataset reprocessed for OMI, which has been adapted for TROPOMI. This uptake assimilation modeling system uses a 3-dimensional global TM5-MP chemical transport model at 1x1 degree resolution as an essential element. As for CO data, negative vertical column values are often observed because of noise, particularly over clean regions with low NO_2 emissions. It is also recommended not to filter these values except for outliers, i.e., vertical columns lower than -0.001 mol/m^2.

For the SO_2 data collection, S5P/TROPOMI performs a one-day return visit of the Earth's surface at an unprecedented 3.5 x 7 km spatial resolution, which allows to investigate fine details and detect much smaller SO_2 areas. Same as for CO and NO_2 data, due to noise, negative vertical column values are often observed especially in clean areas with low SO_2 emissions. It is recommended not to filter these negative values except for outliers, i.e., vertical columns lower than -0.001 mol/m^2.

For the period before the lockdown, the period right before the outbreak occurred, namely 2 months at the end of 2019, was selected. For the period after the lockdown, the closest period when the impact of the pandemic was starting to get heavy and restrictions began was chosen. The period was chosen right after the Nowruz, Persian New Year in Iran because at that time there was a lot of activity and it was feared that it would not be representative. The data period ranged from 1 October 2019 to 1 December 2019 represented a period before the outbreak and from 25 March to 31 May 2020 represented a period during the COVID-19 lockdown as the local activity restrictions started around that period. Other data used included open-source administrative boundary data of Iran and Tehran Province.

Methods

The air pollution distribution pattern analysed in the study were measured using Sentinel-5P data in the period as previously described. Carbon Monoxide (CO), Nitrogen Dioxide (NO_2) and Sulphur Dioxide (SO_2) are the main pollutants in the air and have a significant impact on human physical and environmental conditions if present in large quantities. That is why these pollutants were chosen to study the effect of social restrictions in Iran on the level of pollutants in the research area.

The distribution of pollutants is obtained by extracting the data using scripts that are available in the Google Earth Engine. In this research, the first band used is CO_column_number_density which describes vertically integrated CO column density. The second band used is NO2_column_number_density which describes vertically integrated NO_2 column density. The third band is SO2_column_number_density which describes vertically integrated SO_2 column density. The measurement units are mol/m2. The datasets used represent the periods before and after the COVID-19 outbreak. Furthermore, the analysis of pollutants was also conducted for the Iranian capital, Tehran, to see more clearly the effect of social restrictions in the country's capital, which is the center of government and citizen activity. After the results were obtained, an analysis was carried out to identify the differences in the distribution of pollutants before and after the outbreak in accordance with the limitation of social activities. The research flowchart is shown in Fig. 1.

RESULTS AND DISCUSSION

Iran

The distribution of Carbon Monoxide (CO) levels in Iran before lockdown is shown for the period from 1 October 2019 to 1 December 2019 and during intensive lockdown from 25 March 2020 to 31 May 2020 (Fig. 2). The period before lockdown represents the time before the COVID-19 outbreak emerged in Iran. CO can originate from incomplete combustion processes, like the ones that occur in vehicle engines, including cars and motorcycles, various other types of engines, trains or industries (Somvanshi et al. 2019).

From Figure 2 it can be seen that in Iran in general there is no significant difference in the CO exposure before
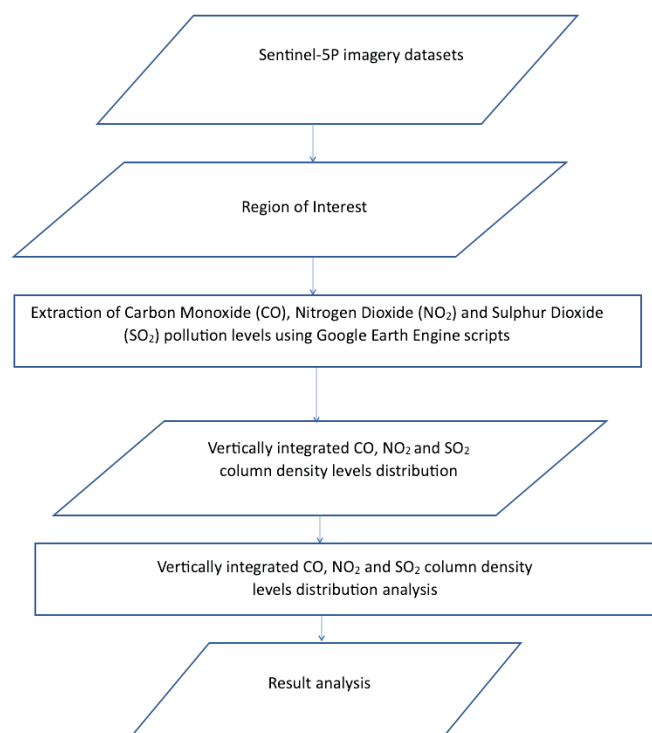
Fig. 1. Flowchart of the CO, NO₂ and SO₂ pollution levels distribution analysis

and after the lockdown that occurred in this region as an effort to control the spread of the virus. Overall, there was a slight increase in CO exposure from 0.0214 mol/m2 to 0.0286 mol/m². In some areas, the pollution level slightly increased from 0.0286 to 0.0357 mol/m², while in the others, the concentration of CO before and after the lockdown stayed the same, namely 0.0286 mol/m².

During the intensive lockdown period, the government began to impose restrictions on social activities such as limitations on travelling between regions and gatherings. The result shows that during the lockdown period from the end of March to the end of July 2020, there was no significant decrease in CO pollution in the Iran region which, in addition to natural levels in the atmosphere, is generally caused by motor vehicles or industrial fumes (TROPOMI 2020). Carbon monoxide and oxygen can be quickly converted to CO_2 in the air. As one of the greenhouse gases associated with global warming, this pollutant is closely related to the temperature: the higher the temperature, the higher the concentration level of CO_2 (NASA 2011).

The climate in Iran varies significantly, the northern part of the country has a cold climate and the western part is mountainous. Both these areas are characterized by low temperatures. This also results in the low CO concentration in these regions before and after the lockdown period compared to the eastern region. The eastern region is a dry desert valley with high temperatures (Wikipedia 2021) and it is marked by higher CO levels before and after the lockdown period. The contrasting climate differences in Iran also affects the differences in greenhouse gas levels over the entire observation period. On the other hand, in a densely populated province such as Tehran where the capital is located, there was a significant decrease in CO concentration during the intensive lockdown period from 0.05 mol/m² to 0.0286 mol/m². This decrease indicates that the lockdown in that area has been effective in reducing the CO exposure due to the limitation of the population activity which resulted in the reduction of anthropogenic emissions in urban areas.

The effect of the intensive lockdown on pollutant concentrations can be seen more clearly for Nitrogen Dioxide (NO_2) levels, which were obtained for Iran from 1 October 2019 to 1 December 2019 and during intensive lockdown from 25 March 2020 to 31 May 2020 (Fig. 3).

NO_2 exists in the atmosphere as a result of anthropogenic activities like burning fossil fuels and biomass as well as natural processes like forest fires and microbiological processes on the ground (TROPOMI 2021).

From the map of NO_2 distribution in Iran, it can be seen that most of the area has NO_2 exposure of 0.0000857 mol/m². From the figure, it can be seen how the level of NO_2 in Iran's big cities decreased during the intensive lockdown period. In the area of Tehran, the capital of Iran, as well as the cities of Qom, Isfahan and Mashhad, it can be seen that the concentration of NO_2 in the city center reaches 0.0002 mol/m². Further away from the city center the concentration of NO_2 decreases successively to 0.000171 and 0.000142 mol/m².

It can also be observed that during the lockdown period there was a decrease in the area that had a high concentration of NO_2. In the main cities of Tehran, Qom, Isfahan and Mashhad, the concentration decreased from 0.0002 to 0.000114 – 0.000171 mol/m². Meanwhile, in other cities such as Ahvaz and Yazd, the value of NO_2 decreased from 0.000142 to 0.000114 mol/m₂. From spatial observation and analysis of the pollutant concentrations, it can be seen that in Iran's big cities there was a decrease in NO_2 pollution during the intensive lockdown period. This was triggered by a reduction in anthropogenic activities in that period such as the burning of fossil fuels which is one of the sources of NO_2.

The next result shows the distribution of Sulphur Dioxide (SO_2) levels in Iran from 1 October 2019 to 1 December 2019 as the period before lockdown and 25 March 2020 to 31 May 2020 as the period during intensive COVID-19 lockdown (Fig. 4). The majority of SO_2 pollutant comes from anthropogenic origin namely from the burning of petroleum and coal, while only a small amount of SO_2 comes from natural sources (TROPOMI 2020).

In the distribution map of SO_2 pollution levels, it can be seen that in the period before the lockdown, high SO_2 concentrations of 0.0005 mol/m² were found in big cities such as Tehran, Isfahan, Qom, Mashhad, Ahvaz and Kerman. Apart from burning fuel, oil and coal, SO_2 exposure also usually occurs in coal-fired power plants such as in South Africa (Shikwambana et al. 2020). The presence of a number of power plants in the region can increase SO_2 exposure.

Furthermore, the map of SO_2 distribution during the intensive lockdown period shows a significant decrease in SO_2 exposure in Iran. It can be observed that the exposure
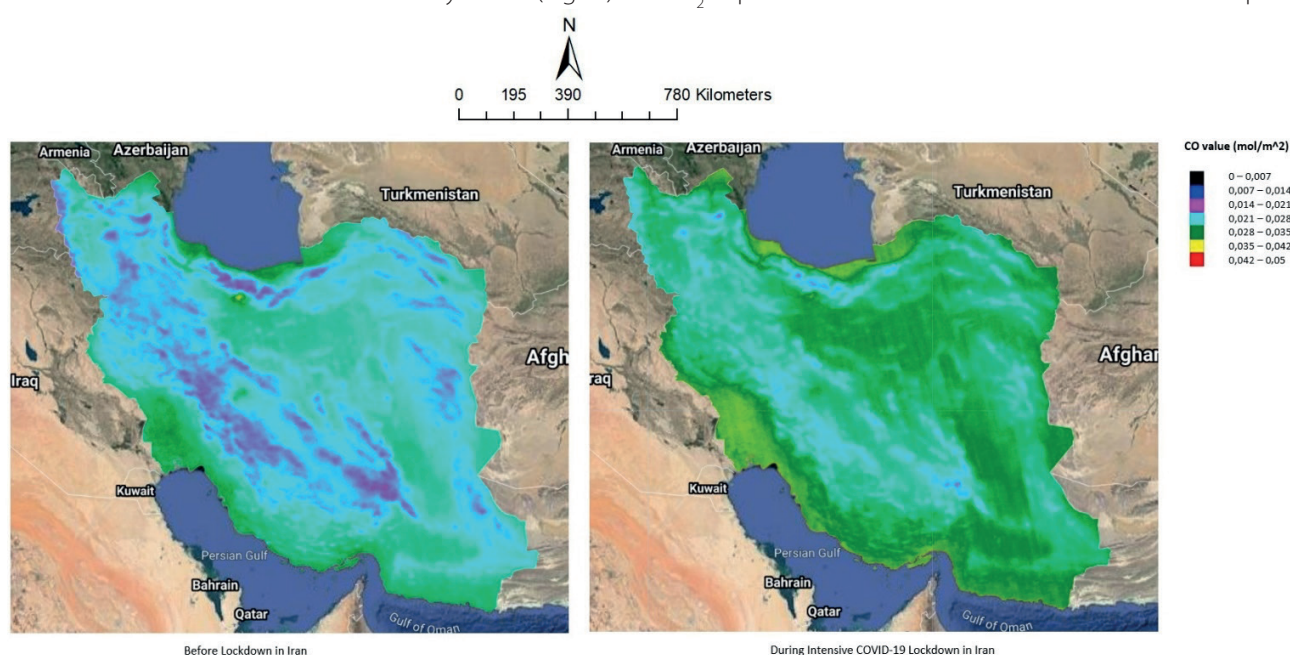

Fig. 2. Distribution of CO levels before and during the COVID-19 lockdown in Iran
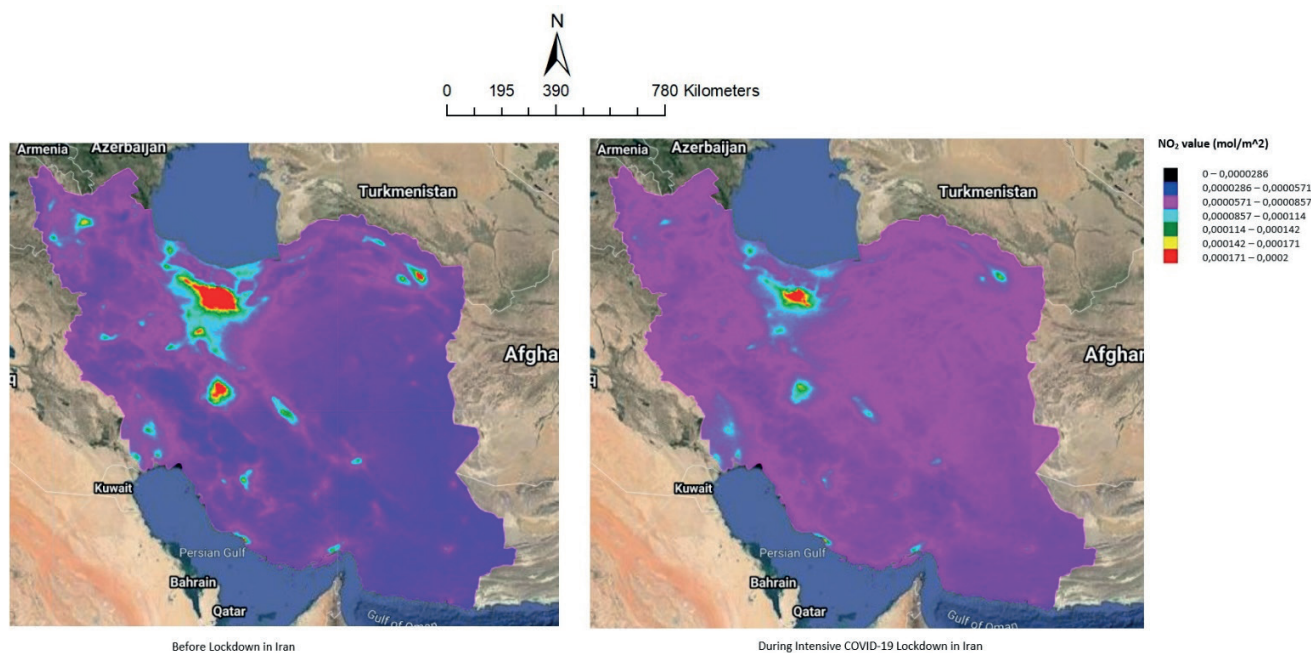
Fig. 3. Distribution of CO levels before and during the COVID-19 lockdown in Iran

level in the areas of Tehran, Qom, Isfahan, which before the lockdown reached up to 0.0005 mol/m^2, decreased after the intensive lockdown to 0.0000714 – 0.000143 mol/m^2. Meanwhile, SO$_2$ concentration in the central and eastern regions of Iran, which originally stood at 0.000143 mol/m^2 for most of the area, decreased to 0 – 0.0000714 mol/m^2. These findings suggest that the period of intensive lockdown along with restrictions on anthropogenic activities in the form of burning oil and coal as one of the sources of this pollutant contributed to a decrease in SO$_2$ pollution in Iran.

Tehran Province

The province of Tehran is the place where the capital city of Iran is located and the richest province in the country. It has more than 12 million inhabitants, making it the most populous region in Iran, about 18% of the country's population resides in the province of Tehran. As the province where the capital is located, Tehran is the commercial center of Iran. Tehran province has over 17.000 industrial units employing approximately 390.000 people,

which is 26% of all units in Iran. The province contains more or less 30% of Iran's economy and comprises 40% of Iran's consumer market (Wikipedia 2021). As a center of economic and business activity, it is very interesting to examine the impact of the lockdown due to the COVID-19 pandemic on the air quality of this busiest province in Iran.

Subsequent results show the level of pollution by CO, NO$_2$ and SO$_2$ in Tehran province before and after the intensive lockdown (Fig. 5, Fig. 6 and Fig. 7). The period for the condition before the outbreak is from 1 October to 1 December 2019 and for the condition after the lockdown is from 25 March to 31 May 2020. As the heart of commercial, business and citizen activities, it can be seen how the level of all types of air pollution in this region is increasing closer to the capital city, Tehran, which is the most populous city in Iran and Western Asia.

As mentioned before, the period chosen for the intensive lockdown starts after 20 March 2020 because on 20 March 2020, there is a celebration of Nowruz or the Persian New Year and pollution related to the effects of this celebration can result in an anomaly in the data. That is
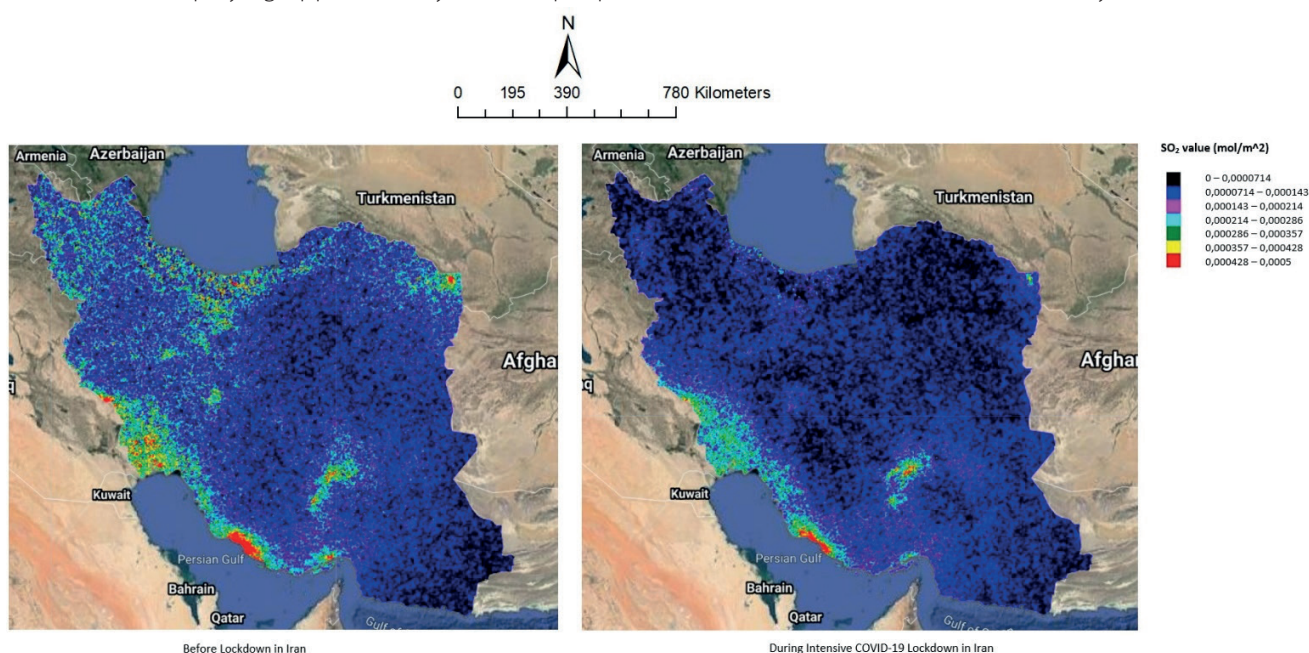

Fig. 4. Distribution of SO$_2$ levels before and during the COVID-19 lockdown in Iran
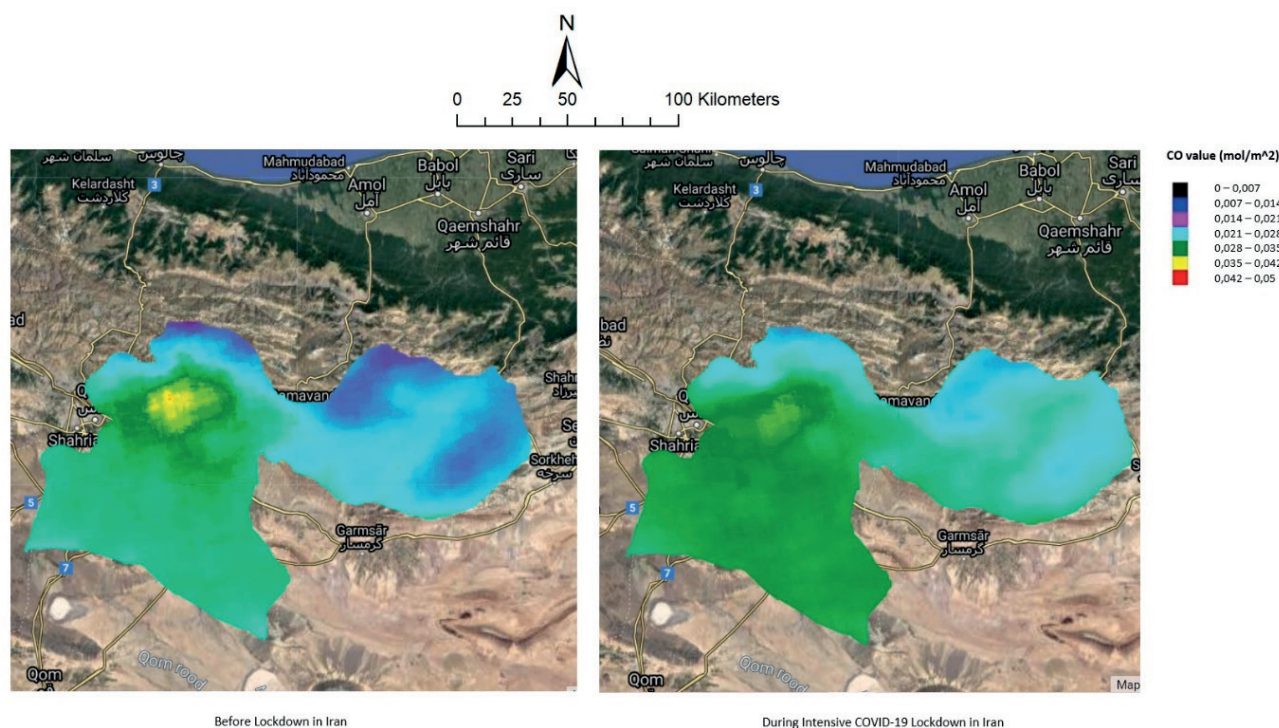
Fig. 5. Distribution of CO levels before and during the COVID-19 lockdown in Tehran Province

why the period chosen for the intensive lockdown is from 25 March to 31 May 2020. Besides restrictions on human activities that have an impact on the emissions from gasoline-powered vehicles, a decrease in CO levels in the air is also related to a decrease in other types of activities such as the metal and building materials industry as well as reduced input from housing sources (Zheng et al., 2018). In another case, the reduction in CO levels can also be due to reduced biomass combustion, biogenic emission and photochemical production (I et al. 2020).

Fig. 5 shows that according to the distribution of air pollution, there was a change in the pattern of CO as it concentrated in the center of Tehran before the outbreak and spread to the surrounding area after the outbreak. Based on CO levels, there was a decrease in pollution in the region.

Before the outbreak occurred, CO pollution levels ranged from 0.014 – 0.0428 mol/m^2, while after the lockdown was enforced, it reduced to 0.014 – 0.036 mol/m^2, which means that there was a decrease in CO levels in Tehran province. In downtown Tehran, it is clearly visible that before the lockdown there was a high CO concentration of 0.043 mol/m^2 which then dropped to 0.036 mol/m^2 after entering the lockdown period.

From Fig. 6, it can be seen how the level of the NO_2 pollutant in this region is increasing closer to the Tehran city center. As with the CO pollutant, the highest concentration of NO_2 is observed closest to downtown Tehran where it reaches 0.0002 mol/m^2. In the period before the lockdown, the region with high NO_2 level covered a wide area in downtown Tehran, occupying up to half of Tehran Province. However, after the lockdown, the area with a NO_2 level of
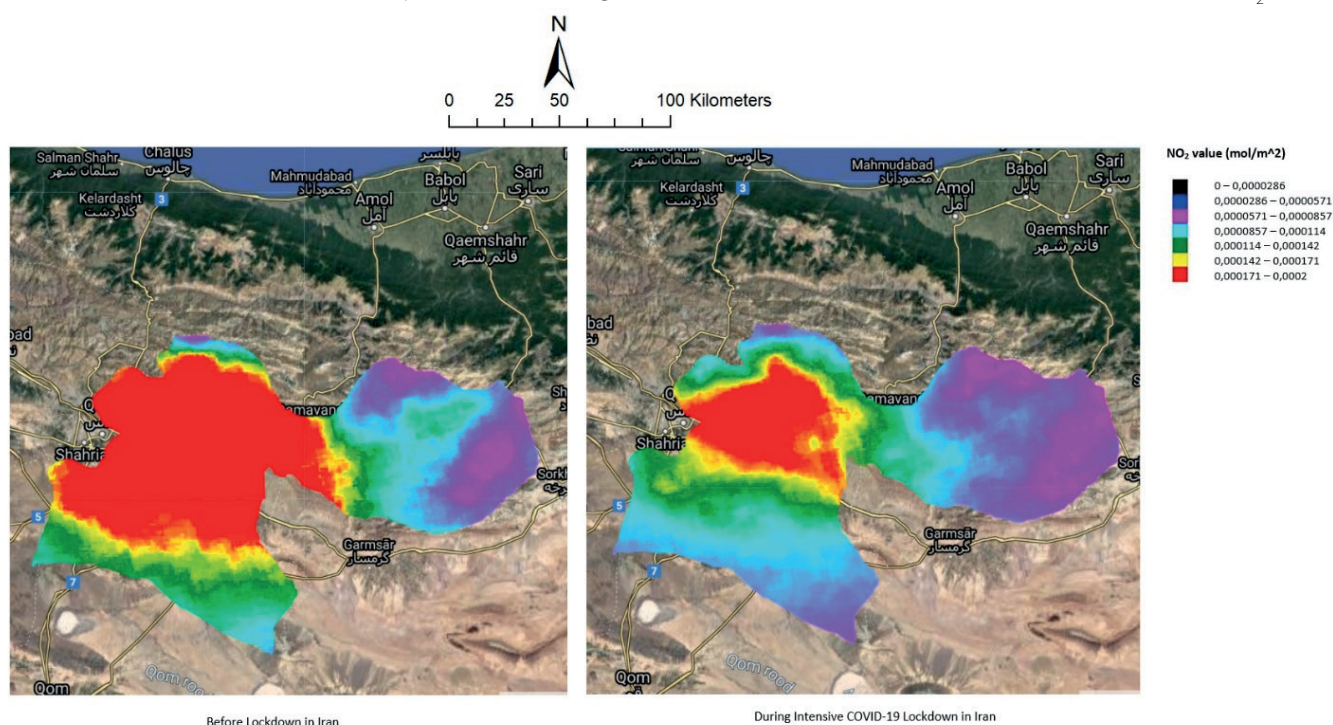

Fig. 6. Distribution of NO_2 levels before and during the COVID-19 lockdown in Tehran Province

0.0002 mol/m^2 decreased and covered only the city center and a few areas around it.

The counties (shahrestan) around Tehran that have high levels of NO$_2$ reaching 0.0002 mol/m^2 include Ray, Eslamshahr, Baharestan, Shahriar, Qarchak, Pakdasht, Pardis, Shemiranat, Qods and Robat Karim. Meanwhile, after the lockdown, these districts experienced a decrease in their NO$_2$ levels from 0.0002 to 0.000142 mol/m^2, except for Tehran, Qods, Eslamshahr and Shahriar which still had high NO$_2$ levels. The decreasing value means that there was a reduction of NO$_2$ levels in the Tehran province due to the limitation of anthropogenic activity that produces this pollutant during the lockdown. In several studies, it was revealed that NOx emissions are mostly associated with activities such as coal combustion at coal-fired power plants, air traffic, road traffic, biomass burning and the N microbial cycle (Adams et al. 2020; Dahlmann et al. 2011; Zong et al. 2018).

From the results that show the level of SO$_2$ pollutant in Tehran province (Fig. 7), it can be seen that its distribution pattern differs from CO and NO$_2$ as it tends to be irregular and evenly distributed in this province. Fig. 7 also shows that the level of SO$_2$ pollution in this province which originally stood at a high value of 0.0005 mol/m^2 decreased to 0.000143 mol/m2. This indicates a decrease in the amount of SO$_2$ after the implementation of a strict lockdown in Tehran province. In some areas of Tehran Province, where originally an SO$_2$ value of 0.000357 mol/m^2 was observed, it decreased to 0 – 0.0000714 mol/m^2 in the period after the lockdown. This change means that there was a significant decrease in SO$_2$ levels in the province of Tehran due to the reduction of anthropogenic activities that produce SO$_2$. Sources of SO$_2$ include burning coal at coal-fired power plants and motor vehicle fumes (Adams et al. 2020; Azimi et al. 2018). Negative values in the obtained pollutant concentrations can arise when the sky conditions are very clear or the pollutant level is very low. This can indeed happen because the lowest range of the minimum SO$_2$ vertical column density in the band used in Sentinel-5P data is a negative value, which indicates a very low or zero density of pollutant molecules (Google Earth Engine 2021).

From the overall results obtained in this study, it can be seen that the Sentinel-5P data is able to present both spatial and temporal distribution of pollutants as well as their concentration in Iran and Tehran Province. From the results, it can be concluded that after the lockdown there was a decrease in the concentration of pollutants in the Iran region compared to the period before the COVID-19 pandemic. Changes in the CO pollutant values are clearly visible in urban areas with high population activity such as Tehran, where CO concentration decreased from 0.05 to 0.0286 mol/m^2, while in other areas it is also influenced by the varying climate in Iran. Meanwhile, for the NO$_2$ pollutant, there was a significant decrease in pollution levels in big cities such as Tehran, Qom, Isfahan and Mashhad, where it reduced from 0.0002 to 0.000114 mol/m^2. Furthermore, for the SO$_2$ pollutant, the pollution levels in Iran's big cities decreased from 0.0005 to 0.0000714 mol/m^2.

Meanwhile for Tehran province, which is the most populous and busiest province in Iran, it can be observed that there was also a decrease in the concentration of pollutants after the lockdown compared to the pre-lockdown period. The CO concentration decreased from 0.043 to 0.036 mol/m^2, while for the NO$_2$ pollutant there was a decrease from 0.0002 to 0.000142 mol/m^2 and for the SO$_2$ pollutant, there was a decrease from 0.0005 to 0.000143 mol/m^2.

CONCLUSION

Based on the results of processing the Sentinel-5P imagery data for Iran and Tehran province, an analysis was done to monitor both spatial and temporal distribution of air pollution, particularly CO, NO$_2$ and SO$_2$ pollutants.

For Iran in general, changes in the concentration of CO are clearly visible in urban areas with high population activity such as Tehran, where there was a decrease from 0.05 to 0.0286 mol/m^2, while for other areas it is also influenced by the varying climate conditions, which affect the level of pollution. For the NO$_2$ pollutant, there was a significant decrease in pollution levels in big cities such as Tehran, Qom, Isfahan and Mashhad from 0.0002 to 0.000114 mol/m^2. For the SO$_2$ pollutant, there was a decrease in pollution levels in
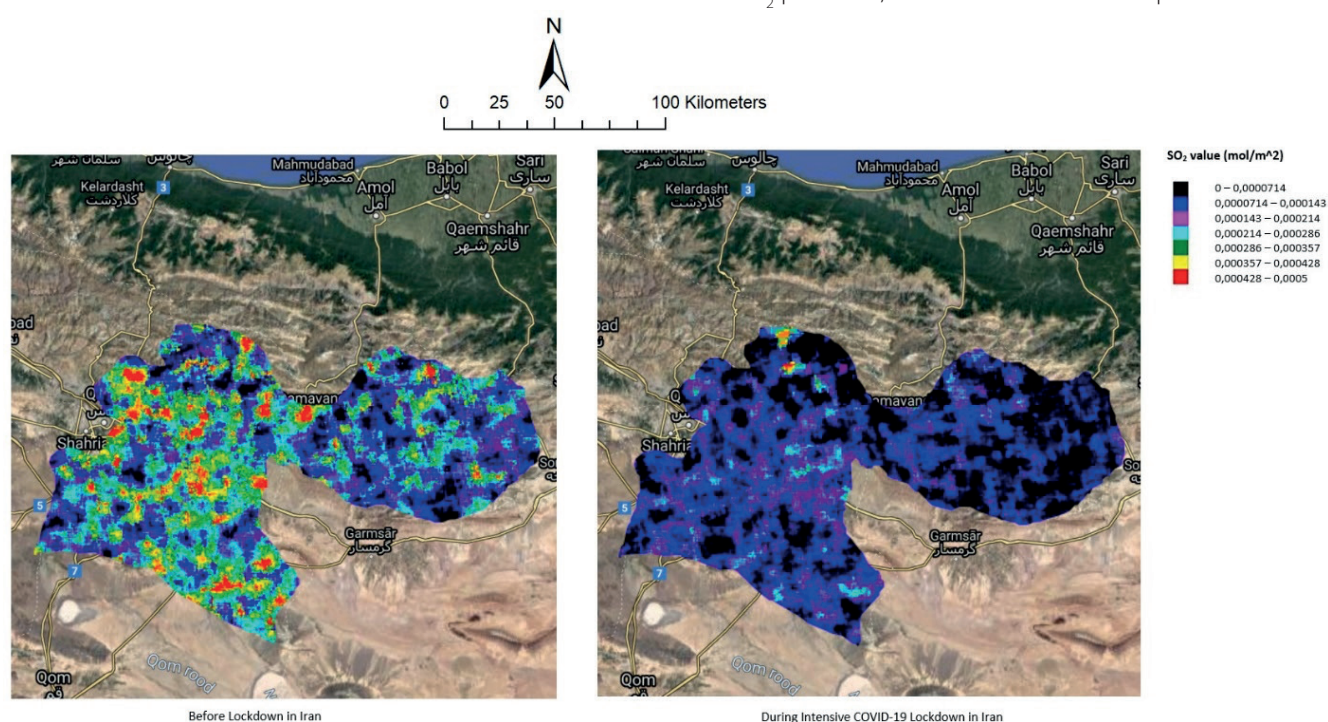

Fig. 7. Distribution of SO$_2$ levels before and during the COVID-19 lockdown in Tehran Province

Iran's big cities from 0.0005 to 0.0000714 mol/m². For Tehran province, which is the most populous and busiest province in Iran, it can be observed that there was also a decrease in the concentration of pollutants after the lockdown compared to the pre-lockdown period. The CO concentration decreased from 0.043 to 0.036 mol/m², while for the NO_2 pollutant there was a decrease from 0.0002 to 0.000142 mol/m² and for the SO_2 pollutant, there was a decrease from 0.0005 to 0.000143 mol/m².

These findings suggest that the period of intensive COVID-19 lockdown contributed to the reduction of CO, NO_2 and SO_2 pollution in Iran, along with the restriction of anthropogenic activities which are the sources of these pollutants. ■

REFERENCES

Adams D., Oh D.H., Kim D.W., Lee C.H. & Oh M. (2020). Prediction of SOx–NOx emission from a coal-fired CFB power plant with machine learning: Plant data learned by deep neural network and least square support vector machine. Journal of Cleaner Production, 270, 122310, DOI: 10.1016/j.jclepro.2020.122310.

Adnan M., Khan S., Kazmi A., Bashir N., & Siddique R. (2020). COVID-19 infection : Origin , transmission , and characteristics of human coronaviruses. Journal of Advanced Research, 24, 91-98, DOI: 10.1016/j.jare.2020.03.005.

Altuğ H., Fuks K.B., Hüls A., Mayer A.K., Tham R., Krutmann J. & Schikowski T. (2020). Air pollution is associated with depressive symptoms in elderly women with cognitive impairment. Environment International, 136(January), DOI: 10.1016/j.envint.2019.105448.

Andersson E.M., Ögren M., Molnár P., Segersson D., & Stockfelt L. (2020). Road traffic noise, air pollution and cardiovascular events in a Swedish cohort. Environmental Research, 109446, DOI: 10.1016/j.envres.2020.109446.

Azimi M., Feng F., & Yang Y. (2018). Air pollution inequality and its sources in SO2 and NOX emissions among Chinese Provinces from 2006 to 2015. Sustainability (Switzerland), 10(2), DOI: 10.3390/su10020367.

Berman J.D., & Ebisu K. (2020). Science of the Total Environment Changes in U . S . air pollution during the COVID-19 pandemic. Science of the Total Environment, 739, 139864, DOI: 10.1016/j.scitotenv.2020.139864.

Chen Y., Wang S., Han W., Xiong Y., Wang W., & Tong L. (2017). A New Air Pollution Source Identification Method Based on Remotely Sensed Aerosol and Improved Glowworm Swarm Optimization. 3454 IEEE JOURNAL OF SELECTED TOPICS IN APPLIED EARTH OBSERVATIONS AND REMOTE SENSING, 10(8), 3454-3464.

Clerbaux C., Bauduin S., Boynard A., Clarisse L., Coheur P., George M., Hadji-lazaro J., Hurtmans D., Safieddine S., Damme M. Van, & Whitburn S. (2017). Observation of Air Pollution over China Using the IASI Thermal Infrared Space Sensor. In Air Pollution in Eastern Asia: An Integrated Perspective, 309-322, DOI: 10.1007/978-3-319-59489-7.

Dahlmann K., Grewe V., Ponater M., & Matthes S. (2011). Quantifying the contributions of individual NOx sources to the trend in ozone radiative forcing. Atmospheric Environment, 45(17), 2860-2868, DOI: 10.1016/j.atmosenv.2011.02.071.

European Space Agency. (2021). Sentinel. https://sentinel.esa.int/web/sentinel/missions/sentinel-5p accessed on June 12th, 2021.

Filonchyk M., Yan H., Yang S., & Lu X. (2017). Detection of aerosol pollution sources during sandstorms in Northwestern China using remote sensed and model simulated data. Advances in Space Research, DOI: 10.1016/j.asr.2017.11.037.

Fu M., Kelly J.A., & Clinch J.P. (2020). Prediction of PM2.5 daily concentrations for grid points throughout a vast area using remote sensing data and an improved dynamic spatial panel model. Atmospheric Environment, 117667, DOI: 10.1016/j.atmosenv.2020.117667.

Google Earth Engine (2020). Sentinel-5P NRTI CO Near Real-Time Carbon Monoxide. Earth Engine Data Catalog.

Huang Y., Organ B., Zhou J.L., Surawski N.C., Hong G., Chan F.C., & Yam Y.S. (2018). Remote sensing of on-road vehicle emissions: mechanism, applications and a case study from Hong Kong. Atmospheric Environment, DOI: 10.1016/j.atmosenv.2018.03.035.

Srivastava I.N., Yarragunta S., Kumar Y., & Mitra D. (2020). Distribution of surface carbon monoxide over the Indian subcontinent: Investigation of source contributions using WRF-Chem. Atmospheric Environment, 243, DOI: 10.1016/j.atmosenv.2020.117838.

Kurata M., Takahashi K., & Hibiki A. (2020). Gender differences in associations of household and ambient air pollution with child health: Evidence from household and satellite-based data in Bangladesh. World Development, 128, 104779, DOI: 10.1016/j.worlddev.2019.104779.

Leifer I., Melton C., Chatfield R., Cui X., Fischer M.L., Fladeland M., Gore W., Hlavka D.L., Iraci L., Marrero J., Ryoo M., Tanaka T., Yates E., & Yorks J. (2019). Air pollution inputs to the Mojave Desert by fusing surface mobile and airborne in situ and airborne and satellite remote sensing: A case study of interbasin transport with numerical model validation. Atmospheric Environment, 117184, DOI: 10.1016/j.atmosenv.2019.117184.

Li J. (Jie), Massa M., Zhang H., & Zhang J. (2019). Air pollution, behavioral bias, and the disposition effect in China. Journal of Financial Economics, xxxx, DOI: 10.1016/j.jfineco.2019.09.003.

Li X., & Zhang X. (2019). Predicting ground-level PM 2 . 5 concentrations in the Beijing-Tianjin- Hebei region : A hybrid remote sensing and machine learning. Environmental Pollution, 249, 735-749, DOI: 10.1016/j.envpol.2019.03.068.

Miller M.R. (2020). Oxidative stress and the cardiovascular effects of air pollution. Free Radical Biology and Medicine, January, DOI: 10.1016/j.freeradbiomed.2020.01.004.

NASA (2011). Effects of Changing the Carbon Cycle. In Earth Observatory

Omrani H., Omrani B., Parmentier B., & Helbich M. (2020). Spatio-temporal data on the air pollutant nitrogen dioxide derived from Sentinel satellite for France. Data in Brief, 28, 105089, DOI: 10.1016/j.dib.2019.105089.

Pacheco H., Díaz-López S., Jarre E., Pacheco H., Méndez W., Zamora-Ledezma E. (2020). NO2 levels after the COVID-19 lockdown in Ecuador: A trade-off between environment and human health. Urban Climate, 34(December), 100674, DOI: 10.1016/j.uclim.2020.100674.

Petrosillo N., Viceconte G., Ergonul O., Ippolito G., & Petersen E. (2020). COVID-19, SARS and MERS: are they closely related? Clinical Microbiology and Infection, DOI: 10.1016/j.cmi.2020.03.026.

Prud G., Dobbin N.A., Sun L., Burnett R.T., Martin R.V, Davidson A., Cakmak S., Villeneuve P.J., Lamsal L.N., Donkelaar A.Van, Peters P.A., & Johnson M. (2013). Comparison of remote sensing and fixed-site monitoring approaches for examining air pollution and health in a national study population. Atmospheric Environment, 80, 161-171, DOI: 10.1016/j.atmosenv.2013.07.020.

Reuters (2020). Iran reports COVID-19 death every four minutes, extends curbs. In Health News.

Rothan H.A., & Byrareddy S.N. (2020). The epidemiology and pathogenesis of coronavirus disease (COVID-19) outbreak. Journal of Autoimmunity, February, 102433, DOI: 10.1016/j.jaut.2020.102433.

Shikwambana L., Mhangara P., Mbatha N. (2020). Trend analysis and first time observations of sulphur dioxide and nitrogen dioxide in South Africa using TROPOMI/Sentinel-5 P data. International Journal of Applied Earth Observation and Geoinformation, 91(September), 102130, DOI: 10.1016/j.jag.2020.102130.

Smit R., Kingston P., Neale D.W., Brown M.K., Verran B. & Nolan T. (2019). Monitoring on-road air quality and measuring vehicle emissions with remote sensing in an urban area. Atmospheric Environment, 218(September), 116978, DOI: 10.1016/j.atmosenv.2019.116978.

Somvanshi S.S., Vashisht A., Chandra U., & Kaushik G. (2019). Delhi Air Pollution Modeling Using Remote Sensing Technique. In Handbook of Environmental Materials Management, 1-27, DOI: 10.1007/978-3-319-58538-3_174-1.

Sun S., Li L., Wu Z., Gautam A., Li J., & Zhao W. (2020). Variation of industrial air pollution emissions based on VIIRS thermal anomaly data. Atmospheric Research, 244(May), 105021, DOI: 10.1016/j.atmosres.2020.105021

Tosepu R., Gunawan J., Effendy D.S., Ahmad L.O.A.I., Lestari H., Bahar H., & Asfian P. (2020). Correlation between weather and Covid-19 pandemic in Jakarta, Indonesia. Science of the Total Environment, 138436, DOI: 10.1016/j.scitotenv.2020.138436.

TROPOMI (2020). Carbon Monoxide. In Data Products

TROPOMI (2020). Nitrogen Dioxide. In Data Products

TROPOMI (2020). Sulphur Dioxide. In Data Products

ul-Haq Z., Tariq S., Ali M. (2015). Atmospheric variability of methane over Pakistan, Afghanistan and adjoining areas using retrievals from SCIAMACHY/ENVISAT. Journal of Atmospheric and Solar-Terrestrial Physics, 135(December), 161-173, DOI: 10.1016/j.jastp.2015.11.002.

Vratolis S., Fetfatzis P., Argyrouli A., Soupiona O., Mylonaki M., & Maroufidis J. (2020). Comparison and complementary use of in situ and remote sensing aerosol measurements in the Athens Metropolitan Area. Atmospheric Environment, 228(March), 117439, DOI: 10.1016/j.atmosenv.2020.117439.

Wan Y., Li Y., Liu C., & Li Z. (2020). Is traffic accident related to air pollution? A case report from an island of Taihu Lake, China. Atmospheric Pollution Research, September 2019, 0-1, DOI: 10.1016/j.apr.2020.02.018

Wang P., Chen K., Zhu S., Wang P., & Zhang H. (2020). Severe air pollution events not avoided by reduced anthropogenic activities during COVID-19 outbreak. Resources, Conservation and Recycling, 158(March), 104814, DOI: 10.1016/j.resconrec.2020.104814.

Wikipedia (2021). Geography of Iran. https://en.wikipedia.org/wiki/Geography_of_Iran accessed on June 14th, 2021.

Wikipedia (2021). Tehran Province. https://en.wikipedia.org/wiki/Tehran_Province accessed on June 15th, 2021.

Zheng B., Chevallier F., Ciais P., Yin Y., Deeter M.N., Worden H.M., Wang Y., Zhang Q., & He K. (2018). Rapid decline in carbon monoxide emissions and export from East Asia between years 2005 and 2016. Environmental Research Letters, 13(044007) , DOI: 10.1088/1748-9326/aab2b3.

Zong Z., Tan Y., Wang X., Tian C., Fang Y., Chen Y., Fang Y., Han G., Li J., & Zhang G. (2018). Assessment and quantification of NOx sources at a regional background site in North China: Comparative results from a Bayesian isotopic mixing model and a positive matrix factorization model. Environmental Pollution, 242, 1379-1386, DOI: 10.1016/j.envpol.2018.08.026.